



## Influence of velocity slip conditions on MHD peristaltic flow of a Prandtl fluid in a non-uniform channel

Kumar, M. A.<sup>1</sup>, Sreenadh, S.<sup>1</sup>, Saravana, R.<sup>2</sup>, Reddy, R. H.\*<sup>3</sup>,  
and Kavitha, A.<sup>3</sup>

<sup>1</sup>*Department of Mathematics, Sri Venkateswara University, India*

<sup>2</sup>*Department of Mathematics, Madanapalle Institute of Technology  
and Science, India*

<sup>3</sup>*School of Advanced Sciences, VIT University, India*

*E-mail: rhreddy@vit.ac.in*

*\*Corresponding author*

### ABSTRACT

The velocity slip effects on MHD peristaltic pumping of a Prandtl fluid in a non-uniform channel is investigated under the assumptions of long wavelength and low Reynolds number. A regular perturbation technique is employed to solve the non-linear system of equations. The velocity field, the axial pressure gradient, the pressure rise and the frictional force over one cycle of the wave length are obtained. The results are discussed graphically. It is noticed that the amplitude of the pressure gradient decreases with increasing the velocity slip parameter further it increases with increasing the Hartmann number.

**Keywords:** MHD, peristaltic pumping, Reynolds number, perturbation technique, non-uniform channel.

## 1. Introduction

Peristaltic transport is a form of fluid transport by means of a progressive wave of area contraction or expansion propagates along the length of a distensible tube. In general, this pumping takes place from a region of lower pressure to higher pressure. It is an inherent property of many of the smooth muscle tubes such as the gastrointestinal tract, sperm transport in the ducts efferentus of the male reproductive tract, movement of ovum in the fallopian tube, the bile duct, the ureter, swallowing of food through esophagus etc.

The principle of peristaltic transport is also exploited in many industrial applications. Sanitary fluid transport, transport of corrosive fluids and blood pumps in heart lung machines are few of these. Since the experimental work of Latham (1996), many investigations on peristalsis under different flow geometries have been presented by various scientists in engineering and applied science.

Peristaltic transport in non-uniform ducts has considerable interest as many pumps in engineering and physiological systems are known to be of non-uniform cross-section. Srivastava and Sinha (1983) studied peristaltic transport of non-Newtonian fluids in non-uniform geometries. Mekheimer (2004) studied the peristaltic flow of blood (modelled as couple stress fluid) under the effect of magnetic field in a non-uniform channel. He noticed that the pressure rise for uniform geometry is much smaller than that for non-uniform geometry. Prasanna Hariharan (2008) investigated the peristaltic transport of non-Newtonian fluid (power law and Bingham fluid model) in a diverging tube with different wall wave forms. Saravana (2011) analyzed the heat transfer on MHD peristaltic transport of a Jeffrey fluid in a non-uniform porous channel with wall properties.

The effect of slip may occur in polymer solutions and molten polymers. Hayat (2012) presented the peristaltic flow of Phan - Thien - Tanner (PTT) fluid in the presence of induced magnetic field and slip conditions. Saravana (2013) discussed the peristaltic transport of an incompressible MHD third order fluid in an inclined asymmetric channel with velocity slip, heat and mass transfer. Vajravelu (2013) studied the peristaltic transport of a conducting Carreau fluid in a non-uniform channel with velocity slip, thermal and concentration jump conditions.

The fluids present in the ducts of a living body can be classified as Newtonian and non-Newtonian fluids based on their behavior. Among several non-Newtonian models, Prandtl fluid model is one of the important models given

by Patel and Timol (2010) for describing biofluids such as blood. Nooreen Sher Akbar. (2012) studied the peristaltic transport of a Prandtl fluid model in an asymmetric channel. Recently, RahmatEllahi. (2014) studied the peristaltic transport of Prandtl nanofluid in a uniform rectangular duct. Very recently, Nadeem (2014) presented the series solution for peristaltic flow of a Prandtl fluid model.

Motivated by these studies, the peristaltic transport of a conducting Prandtl fluid in a non-uniform channel with slip effects is studied under long wavelength and low Reynolds number assumptions. The velocity field, the axial pressure gradient, the volume flux, the pressure rise and the frictional force over one cycle of the wave length are obtained and the results are presented graphically.

## 2. Mathematical Formulation

Consider the flow of a Prandtl fluid in a two dimensional symmetric non-uniform channel. The flow is induced by periodic peristaltic wave propagation of constant speed  $c$ . A uniform magnetic field  $B_0$  is applied in the transverse direction to the flow. The fluid is considered to be of small electrical conductivity so that the magnetic Reynolds number is very small and hence the induced magnetic field is negligible in comparison with the applied magnetic field. The external electric field is zero and the electric field due to polarization of charges is also negligible. Fig. 1 represents the physical model of the flow under consideration.

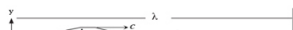


Figure 1: Physical model.

The wall deformation due to the infinite train of peristaltic waves is represented by

$$Y = H(X, t) = d(X) + a \cos \frac{2\pi}{\lambda} (X - ct) \quad (1)$$

where  $d(X) = d + mX$ ;  $m \ll 1$  represents linear non-uniformity of the channel,  $a$  is the amplitude,  $\lambda$  is the wavelength,  $d$  is the mean half width of the channel,  $m$  is the dimensional non-uniformity of the channel.

We introduce a wave frame of reference  $(x, y)$  moving with the velocity  $c$  in which the motion becomes independent of time when the channel length is an integral multiple of the wave length and the pressure difference across at the ends of the channel is a constant. The transformation from the fixed frame of reference  $(X, Y)$  to the wave frame of reference  $(x, y)$  is given by

$$x = X - ct, \quad y = Y, \quad u = U - c, \quad v = V, \quad p(x) = P(X, t) \quad (2)$$

where  $(u, v)$  and  $(U, V)$  are the velocity components,  $p$  and  $P$  are the pressures in the wave and fixed frames of reference respectively.

The constitutive equation for a Prandtl fluid (following Patel and Timol (2010))

$$\tau = \frac{A \sin^{-1} \left( \frac{1}{C} \left( \left( \frac{\partial u}{\partial y} \right)^2 + \left( \frac{\partial v}{\partial x} \right)^2 \right)^{\frac{1}{2}} \right)}{\left( \left( \frac{\partial u}{\partial y} \right)^2 + \left( \frac{\partial v}{\partial x} \right)^2 \right)^{\frac{1}{2}}} \frac{\partial u}{\partial y} \quad (3)$$

in which  $A$  and  $C$  are material constants of Prandtl fluid model. The equations governing the flow field, in the wave frame of reference are

$$\frac{\partial u}{\partial x} + \frac{\partial v}{\partial y} = 0 \quad (4)$$

$$\rho \left( u \frac{\partial u}{\partial x} + v \frac{\partial u}{\partial y} \right) = -\frac{\partial p}{\partial x} + \frac{\partial \tau_{xx}}{\partial x} + \frac{\partial \tau_{xy}}{\partial y} - \sigma B_0^2 (u + c) \quad (5)$$

$$\rho \left( u \frac{\partial v}{\partial x} + v \frac{\partial v}{\partial y} \right) = -\frac{\partial p}{\partial y} + \frac{\partial \tau_{yx}}{\partial x} + \frac{\partial \tau_{yy}}{\partial y} \quad (6)$$

where  $\rho$  is the density,  $\sigma$  is the electrical conductivity and  $B_0$  is the intensity of the magnetic field acting along the  $y$ -axis and the induced magnetic field is assumed to be negligible.

Due to symmetry, the boundary conditions for the velocity are

$$\frac{\partial u}{\partial y} = 0 \quad \text{at} \quad y = 0 \quad (7)$$

$$u + \beta_1 \tau_{xy} = -1 \quad \text{at} \quad y = H \quad (\text{following Vajravelu (2013) in wave frame of reference}) \quad (8)$$

In order to write the governing equations and the boundary conditions in dimensionless form, the following non-dimensional quantities are introduced.

$$\begin{aligned} \bar{x} &= \frac{x}{\lambda}, & \bar{y} &= \frac{y}{d}, & \bar{u} &= \frac{u}{c}, & \bar{v} &= \frac{v}{c\delta}, & \phi &= \frac{a}{d}, & \delta &= \frac{d}{\lambda}, & \bar{p} &= \frac{pd^2}{\mu c \lambda}, & h &= \frac{H}{d}, \\ \bar{t} &= \frac{ct}{\lambda}, & \bar{\tau}_{xx} &= \frac{d}{\mu c} \tau_{xx}, & \bar{\tau}_{xy} &= \frac{d}{\mu c} \tau_{xy}, & \bar{\tau}_{yy} &= \frac{d}{\mu c} \tau_{yy}, & Re &= \frac{\rho dc}{\mu}, & \alpha &= \frac{A}{\mu C}, \\ \beta &= \frac{\alpha c^2}{6C^2 d}, & \bar{\beta}_1 &= \frac{\beta_1}{d}, & \bar{m} &= \frac{m\lambda}{d}, & \bar{q} &= \frac{q}{dc} \end{aligned} \quad (9)$$

In view of equation (9), the equations (4) - (6), after dropping bars, reduce to

$$\frac{\partial u}{\partial x} + \frac{\partial v}{\partial y} = 0 \quad (10)$$

$$Re\delta \left( u \frac{\partial u}{\partial x} + v \frac{\partial u}{\partial y} \right) = -\frac{\partial p}{\partial x} + \delta \frac{\partial \tau_{xx}}{\partial x} + \frac{\partial \tau_{xy}}{\partial y} - M^2(u + 1) \quad (11)$$

$$Re\delta^3 \left( u \frac{\partial v}{\partial x} + v \frac{\partial v}{\partial y} \right) = -\frac{\partial p}{\partial y} + \delta^2 \frac{\partial \tau_{yx}}{\partial x} + \delta \frac{\partial \tau_{yy}}{\partial y} \quad (12)$$

where  $M^2 = \frac{\sigma d^2 B_0^2}{\mu}$  is the square of the Hartmann number.  $Re$  is the Reynolds number,  $\delta$  is the wave number,  $\beta_1$  is the non-dimensional velocity slip parameter,  $\alpha$  and  $\beta$  are Prandtl parameters.

Under the assumptions of long wave length and low Reynolds number, from equations (11) and (12), we get

$$\frac{\partial p}{\partial x} = \frac{\partial \tau_{xy}}{\partial y} - M^2(u + 1) \quad (13)$$

$$\frac{\partial p}{\partial y} = 0 \quad (14)$$

where  $\tau_{xy} = \alpha \frac{\partial u}{\partial y} + \beta \left( \frac{\partial u}{\partial y} \right)^3$

The corresponding dimensionless boundary conditions in wave frame of reference are given by

$$\frac{\partial u}{\partial y} = 0 \quad \text{at} \quad y = 0 \quad (15)$$

$$u = -1 - \beta_1 \tau_{xy} \quad \text{at} \quad y = h = 1 + mx + \phi \cos 2\pi x \quad (16)$$

The volume flow rate  $q$  in a wave frame of reference is given by

$$q = \int_0^{h(x)} u dy. \quad (17)$$

The instantaneous flux  $Q(X, t)$  in a fixed frame is

$$Q(X, t) = \int_0^h U dY = \int_0^h (u + 1) dy = q + h. \quad (18)$$

The time average flux  $\bar{Q}$  over one period of the peristaltic wave is

$$\bar{Q} = \frac{1}{T} \int_0^T Q dt = \int_0^1 (q + h) dx = q + 1. \quad (19)$$

### 3. Perturbation solution

The equation (13) is non-linear and its closed form solution is not possible. Hence we linearize this equation in terms of small Prandtl parameter  $\beta$ . So we expand  $u$ ,  $\frac{dp}{dx}$  and  $q$  as

$$\begin{aligned} u &= u_0 + \beta u_1 + O(\beta^2) \\ \frac{dp}{dx} &= \frac{dp_0}{dx} + \beta \frac{dp_1}{dx} + O(\beta^2) \\ q &= q_0 + \beta q_1 + O(\beta^2) \end{aligned} \quad (20)$$

Substituting (20) in the equation (13) and in the boundary conditions (15) and (16) and then equating the coefficients of like powers of  $\beta$  and neglecting the terms of  $\beta^2$  and higher order, we get the following system of equations of different orders:

**Zeroth order system**

The governing equation is

$$\frac{dp_0}{dx} = \alpha \frac{\partial^2 u_0}{\partial y^2} - M^2(u_0 + 1) \tag{21}$$

The respective boundary conditions are

$$\frac{\partial u_0}{\partial y} = 0 \quad \text{at} \quad y = 0 \tag{22}$$

$$u_0 = -1 - \beta_1 \alpha \frac{\partial u_0}{\partial y} \quad \text{at} \quad y = h \tag{23}$$

Solving the equation (21) by using the boundary conditions (22) and (23), we get

$$u_0 = \frac{1}{N^2 \alpha} \frac{dp_0}{dx} \left( \frac{\cosh Ny}{(\cosh Nh + N\alpha\beta_1 \sinh Nh)} - 1 \right) - 1 \tag{24}$$

and the volume flow rate is given by

$$q_0 = \int_0^h u_0 dy = \frac{1}{N^3 \alpha} \left( \frac{dp_0}{dx} \right) \left[ \frac{\sinh Nh (1 - N^2 h \alpha \beta_1) - Nh \cosh Nh}{\cosh Nh + N\alpha\beta_1 \sinh Nh} \right] - h \tag{25}$$

From equation (25), we get

$$\frac{dp_0}{dx} = N^3 \alpha \left[ \frac{(q_0 + h) \cosh Nh + N\alpha\beta_1 \sinh Nh}{\sinh Nh (1 - N^2 h \alpha \beta_1) - Nh \cosh Nh} \right] \tag{26}$$

where  $N = \frac{M}{\sqrt{\alpha}}$

**First order system**

The governing equation is

$$\frac{dp_1}{dx} = \alpha \frac{\partial^2 u_1}{\partial y^2} + \frac{\partial}{\partial y} \left[ \left( \frac{\partial u_0}{\partial y} \right)^3 \right] - M^2 u_1 \tag{27}$$

$$\frac{\partial u_1}{\partial y} = 0 \quad \text{at} \quad y = 0 \tag{28}$$

$$u_1 = -\alpha\beta_1 \frac{\partial u_1}{\partial y} - \beta_1 \left( \frac{\partial u_0}{\partial y} \right)^3 \quad \text{at} \quad y = h \tag{29}$$

Solving the equation (27) by using the equation (24) and the boundary conditions (28) and (29), we get

$$u_1 = \frac{1}{N^2\alpha} \frac{dp_1}{dx} \left[ \frac{\cosh Ny}{\cosh Nh + N\alpha\beta_1 \sinh Nh} - 1 \right] + \left[ \frac{\sinh Ny}{16N^3\alpha^4 (\cosh Nh + N\alpha\beta_1 \sinh Nh)^3} y + \frac{\beta_1 \sinh^3 Ny}{12N^3\alpha^3 (\cosh Nh + N\alpha\beta_1 \sinh Nh)^4} + \frac{B}{384N^4\alpha^4 (\cosh Nh + N\alpha\beta_1 \sinh Nh)^4} \right] \left( \frac{dp_0}{dx} \right)^3 \quad (30)$$

where

$$B = -3 \cosh Nh - 3 \cosh^3 Nh + 3 \cosh Nh(4hN^2\alpha\beta_1 + 2 \cosh^2 Ny - 3 \sinh^2 Nh + 2 \sinh^2 Ny) + 3N(3\alpha\beta_1 + 4h) \sinh Nh - 9N\alpha\beta_1 \sinh 3Nh + 6N\alpha\beta_1(\cosh^2 Ny + \sinh^2 Ny) \sinh Nh$$

and the volume flow rate is given by

$$q_1 = \int_0^h u_1 dy = \frac{1}{N^3\alpha} \frac{dp_1}{dx} \left[ \frac{\sinh Nh - Nh(\cosh Nh + N\alpha\beta_1 \sinh Nh)}{(\cosh Nh + N\alpha\beta_1 \sinh Nh)} \right] + \left( \frac{dp_0}{dx} \right)^3 B_1 \quad (31)$$

where  $B_1 = \frac{12hN - 8 \sinh 2hN + \sinh 4hN + 24N\alpha\beta_1 \sinh^4 Nh}{192N^5\alpha^4(\cosh Nh + N\alpha\beta_1 \sinh Nh)^4}$

From equation (31), we have

$$\frac{dp_1}{dx} = \frac{N^3\alpha (\cosh Nh + N\alpha\beta_1 \sinh Nh)}{(\sinh Nh(1 - N^2h\alpha\beta_1) - Nh \cosh Nh)} \left( q_1 - B_1 \left( \frac{dp_0}{dx} \right)^3 \right) \quad (32)$$

Substituting the equations (26) and (32) in the relation  $\frac{dp_0}{dx} = \frac{dp}{dx} - \beta \frac{dp_1}{dx}$  and neglecting the terms greater than  $O(\beta)$ , we get

$$\frac{dp}{dx} = \frac{N^3\alpha (\cosh Nh + N\alpha\beta_1 \sinh Nh) \left( (q+h) - \beta B_1 \left( \frac{N^3\alpha(q+h)(\cosh Nh + N\alpha\beta_1 \sinh Nh)}{\sinh Nh(1 - N^2h\alpha\beta_1) - Nh \cosh Nh} \right)^3 \right)}{(\sinh Nh(1 - N^2h\alpha\beta_1) - Nh \cosh Nh)} \quad (33)$$

The dimensionless pressure rise and frictional force per one wavelength in the wave frame are defined, respectively as

$$\Delta P = \int_0^1 \frac{dp}{dx} dx \quad (34)$$



and

$$F = \int_0^1 h \left( -\frac{dp}{dx} \right) dx. \tag{35}$$

### 4. Result and discussion

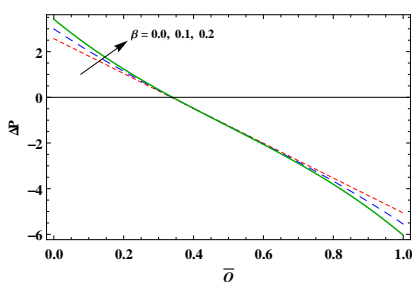


Figure 2: The variation of  $\Delta P$  with  $\bar{Q}$  for different values of  $\beta$  with  $M = 1$ ,  $\beta_1 = 0.1$ ,  $\alpha = 1.5$ ,  $\phi = 0.6$  and  $m = 0.1$ .

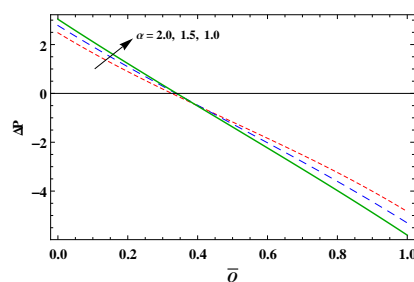


Figure 3: The variation of  $\Delta P$  with  $\bar{Q}$  for different values of  $\alpha$  with  $M = 1$ ,  $\beta_1 = 0.1$ ,  $\beta = 0.1$ ,  $\phi = 0.6$  and  $m = 0.1$ .

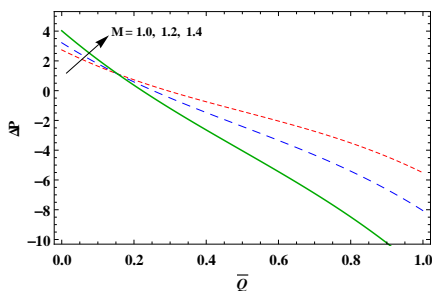


Figure 4: The variation of  $\Delta P$  with  $\bar{Q}$  for different values of  $M$  with  $\alpha = 0.5$ ,  $\beta_1 = 0.05$ ,  $\beta = 0.1$ ,  $\phi = 0.6$  and  $m = 0.1$ .

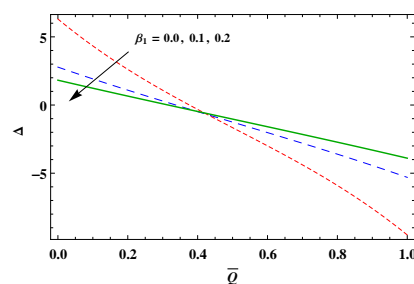


Figure 5: The variation of  $\Delta P$  with  $\bar{Q}$  for different values of  $\beta_1$  with  $M = 1$ ,  $\alpha = 1.5$ ,  $\beta = 0.1$ ,  $\phi = 0.6$  and  $m = 0.1$ .

From equation (34) we have calculated the pressure difference as a function of  $\bar{Q}$ . The variation of  $\Delta P$  with  $\bar{Q}$  for different values of Prandtl parameters  $\beta$  and  $\alpha$ , slip parameter  $\beta_1$ , Hartmann number  $M$  and the non-uniform parameter  $m$  are shown from Figs. 2 to 6. From Fig. 2 we observe that for the peristaltic pumping ( $\Delta P > 0$ ), the flux  $\bar{Q}$  increases with increasing the Prandtl parameter  $\beta$ , for free pumping ( $\Delta P = 0$ ) no variation is found in the flux whereas in the co-pumping ( $\Delta P < 0$ ) the flux decreases with an increase in  $\beta$  and from Fig. 3 opposite behaviour is noticed for another Prandtl parameter  $\alpha$ . In Fig. 4 we find that the pumping curves coincide at the point  $\bar{Q} = 0.15$ , the pressure rise  $\Delta P$  increases with increasing  $M$  when  $\bar{Q} < 0.15$  and when  $\bar{Q} > 0.15$  the

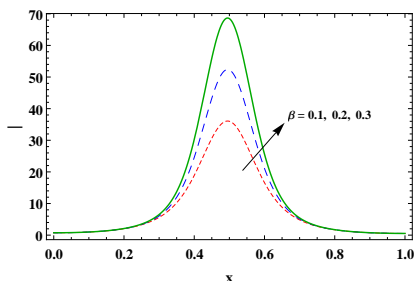


Figure 6: The variation of  $\frac{dp}{dx}$  with  $x$  for different values of  $\beta$  with  $M = 1$ ,  $\beta_1 = 0.1$ ,  $\alpha = 1$ ,  $\phi = 0.5$ ,  $m = 0.1$  and  $\bar{Q} = -1$ .

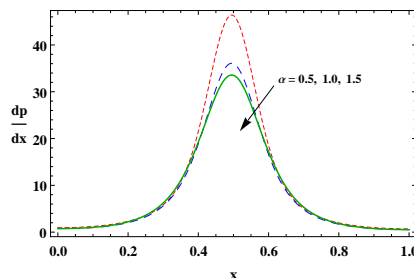


Figure 7: The variation of  $\frac{dp}{dx}$  with  $x$  for different values of  $\alpha$  with  $M = 1$ ,  $\beta_1 = 0.1$ ,  $\beta = 0.1$ ,  $\phi = 0.5$ ,  $m = 0.1$  and  $\bar{Q} = -1$ .

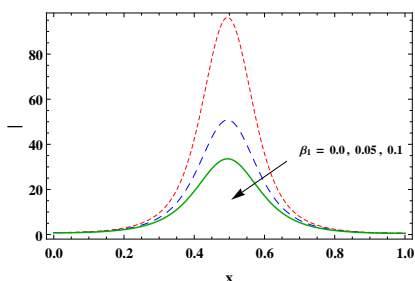


Figure 8: The variation of  $\frac{dp}{dx}$  with  $x$  for different values of  $\beta_1$  with  $M = 1$ ,  $\alpha = 1.5$ ,  $\beta = 0.1$ ,  $\phi = 0.5$ ,  $m = 0.1$  and  $\bar{Q} = -1$ .

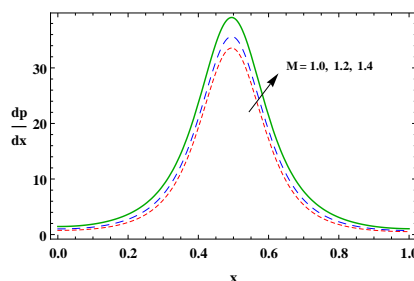


Figure 9: The variation of  $\frac{dp}{dx}$  with  $x$  for different values of  $M$  with  $\beta_1 = 0.1$ ,  $\alpha = 1.5$ ,  $\beta = 0.1$ ,  $\phi = 0.5$ ,  $m = 0.1$  and  $\bar{Q} = -1$ .

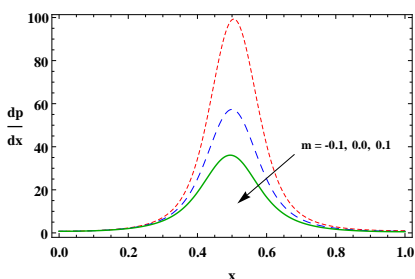


Figure 10: The variation of  $\frac{dp}{dx}$  with  $x$  for different values of  $m$  with  $\beta_1 = 0.1$ ,  $\alpha = 1.5$ ,  $\beta = 0.1$ ,  $\phi = 0.5$ ,  $M = 1$  and  $\bar{Q} = -1$ .

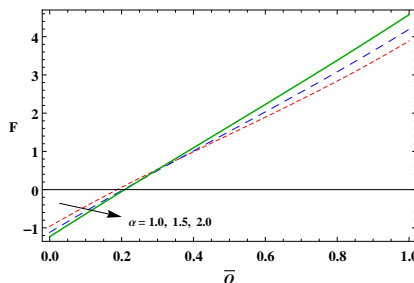


Figure 11: The variation of  $F$  with  $\bar{Q}$  for different values of  $\alpha$  with  $M = 1$ ,  $\beta_1 = 0.1$ ,  $\beta = 0.1$ ,  $\phi = 0.6$  and  $m = 0.1$ .

pressure rise decreases with increasing  $M$ . From Fig. 5 we observe that the  $\bar{Q}$  decreases with an increase in  $\beta_1$  in the pumping region, whereas in the co-pumping region  $\bar{Q}$  increases with an increase in  $\beta_1$ . Equation (33) gives the expression for the axial pressure gradient  $\frac{dp}{dx}$  in terms of  $x$ . Pressure gradient

Influence of velocity slip conditions on MHD peristaltic flow

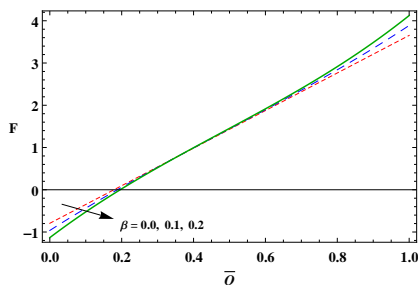


Figure 12: The variation of  $F$  with  $\bar{Q}$  for different values of  $\beta$  with  $M = 1$ ,  $\beta_1 = 0.1$ ,  $\alpha = 1$ ,  $\phi = 0.6$  and  $m = 0.1$ .

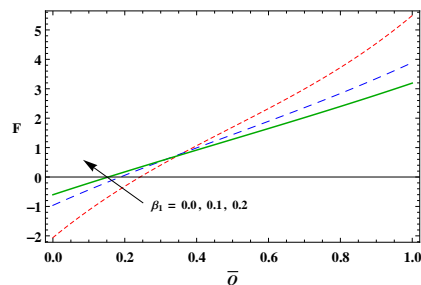


Figure 13: The variation of  $F$  with  $\bar{Q}$  for different values of  $\beta_1$  with  $M = 1$ ,  $\beta = 0.1$ ,  $\alpha = 1$ ,  $\phi = 0.6$  and  $m = 0.1$ .

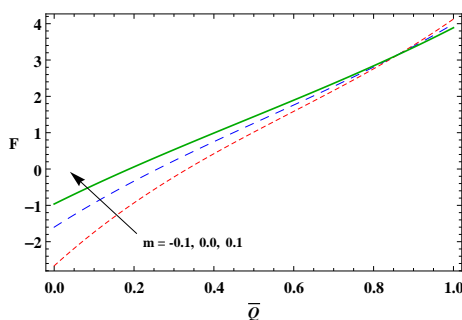


Figure 14: The variation of  $F$  with  $\bar{Q}$  for different values of  $m$  with  $M = 1$ ,  $\beta_1 = 0.1$ ,  $\beta = 0.1$ ,  $\alpha = 1$  and  $\phi = 0.6$ .

profiles are plotted in Figs. 6-10 to study the effects of  $\beta$ ,  $\alpha$ ,  $\beta_1$ ,  $M$  and  $m$ . From Fig. 6 we notice that the pressure gradient increases with the increase of  $\beta$ . In Fig. 7 we observe that the pressure gradient decreases by increasing  $\alpha$ . From Fig. 8 and Fig. 9 we notice that as  $\beta_1$  increases, the magnitude of the pressure gradient decreases whereas the magnitude increases by increasing the Hartmann number. In Fig. 10 we see that as  $m$  increases, the magnitude of the pressure gradient decreases.

Finally from equation (35), we have calculated frictional force  $F$  as a function of  $\bar{Q}$  for  $\alpha$  and  $\beta$  are depicted in Figs.11 to 14. From Figs. 11 and 12, it is found that friction force decreases and then increases with an increase in  $\alpha$  and  $\beta$ . From Figs. 13 and 14, it is found that friction force increases for smaller values of  $\bar{Q}$  and then decreases with an increase in  $\beta_1$  and  $m$  for the higher values of  $\bar{Q}$ . In general, figures 11 to 14 shows that the frictional force  $F$  has opposite behavior compared to pressure rise  $\Delta P$ .

## 5. Concluding Remarks

The present paper deals with the peristaltic transport of a Prandtl fluid in presence of magnetic field and velocity slip conditions at walls of a non-uniform channel. The flow is investigated in a wave frame of reference moving with the velocity of the wave. By using a perturbation method, the expressions for velocity, pressure gradient, pressure rise and frictional force per wave length are obtained. The features of the flow characteristics are analyzed through graphs and the results are discussed in detail. Some of the interesting findings are made from the analysis

- The amplitude of the pressure gradient decreases with increasing the velocity slip parameter  $\beta$  further it increases with increasing the Hartmann number  $M$ .
- The frictional force has the opposite behavior when compared with the pressure rise.
- The results of no slip condition can be observed by considering  $\beta_1 = 0$

## References

- Hayat, T., N. S. H. A. A. (2012). Peristaltic motion of phan-thien-tanner fluid in the presence of slip condition. *Journal of Biorheology*, 25(1):8–17.
- Latham, T. (1996). *Fluid motion in a peristaltic pump*. PhD thesis, Massachusetts Institute of Technology, Cambridge, USA.
- Mekheimer, K. S. (2004). Peristaltic flow of blood under the effect of magnetic field in a non-uniform channels. *Appl. Math. Comput.*, 153:510–523.
- Nadeem, S., R. A. E. R. (2014). Series solution of three dimensional peristaltic flow of prandtl fluid in a rectangular channel. *JAppl Mech Eng.*, 3:139.
- Nooreen Sher Akbar., Nadeem, S. C. L. (2012). Peristaltic flow of a prandtl fluid model in an asymmetric. *International Journal of the Physical Sciences.*, 7(5):687–695.
- Patel, M. and Timol, M. (2010). The stress strain relationship for viscous-inelastic non-newtonian fluids. *Int. J. Phys. Sci.*, 6(12):79–93.
- Prasanna Hariharan, Seshadri, V. R. K. B. (2008). Peristaltic transport of non-newtonian fluid in a diverging tube with different wave forms. *Mathematical and Computer Modelling*, 48:998–1017.

- RahmatEllahi., Arshad Riaz., N. S. (2014). Peristaltic flow of a prandtl fluid model in an asymmetric. *Appl Nanosci.*, 4:753–760.
- Saravana, R., H. R. R. S. S. V. S. K. A. (2013). Influence of slip, heat and mass transfer on the peristaltic transport of a third order fluid in an inclined asymmetric channel. *Int. J. of Appl. Math and Mech*, 9(11):51–86.
- Saravana, R., S. S. V. S. H. R. R. K. A. (2011). Influence of slip conditons, wall properties and heat transfer on mhd peristaltic transport of a jeffrey fluid in a non-uniform channel. *International Journal of Innovative Technology and Creative Engineering*, 1(2):10–24.
- Srivastava, L. M., S. V. P. and Sinha, S. N. (1983). Peristaltic transport of a physiological fluid: Part i. flow in non-uniform geometry. *Biorheol.*, 20:153–166.
- Vajravelu, K., S. S. S. R. (2013). Combined influence of velocity slip, temperature and concentration jump conditions on mhd peristaltic transport of a carreau fluid in a non-uniform channel. *Applied Mathematics and Computation*, 225:656–676.